SPEKTRA: Jurnal Fisika dan Aplikasinya
Volume 10, Issue 2, August 2025
Homepage: doi.org/10.21009/SPEKTRA

DOI: doi.org/10.21009/SPEKTRA.102.03

Analyzing the Influence of Bedrock Geometry on Ambient Vibration Using HVSR and Particle Dynamics

Hanum Fazah[1,*], Yudi Rosandi[2]

[1] *Physics Department, Faculty of Mathematics and Natural Sciences, Universitas Padjajaran, Jl.Raya Bandung-Sumedang KM21, Kabupaten Sumedang, 45633, West Java, Indonesia*
[2] *Geophysics Department, Faculty of Mathematics and Natural Sciences, Universitas Padjajaran, Jl.Raya Bandung-Sumedang KM21, Kabupaten Sumedang, 45633, West Java, Indonesia*

*Corresponding Author Email: hanum24001@mail.unpad.ac.id

Received: 10 May 2025
Revised: 30 July 2025
Accepted: 8 August 2025
Online: 30 August 2025
Published: 31 August 2025

SPEKTRA: Jurnal Fisika dan Aplikasinya
p-ISSN: 2541-3384
e-ISSN: 2541-3392

ABSTRACT

Ground vibration signals recorded by low-frequency multi-channel geophones provide information about the physical characteristics of a medium. Using the passive seismic method, vibrations are measured in three channels, i.e. horizontal and vertical directions. Since the characteristics of mediums, such as sediment thickness and soil hardness, are contained in low-amplitude ambient vibrations, further data selection is required to remove spikes in the signals induced by active sources. This work is necessary to reveal the characteristics that reflect the mediums' physical condition from the signal. Conventionally, signal processing is based on the Horizontal-to-Vertical Signal Ratio (HVSR) calculation. The information obtained, such as sediment thickness and sub-surface shear velocity (V_{s30}), as well as the amplification factor and seismic vulnerability, are crucial for geotechnical applications. This data can be extracted from HVSR analysis. However, a complete understanding of the complex vibration signal shape related to the medium and local geological conditions is not fully understood. To gain a deeper understanding of the mechanism, numerical modeling is performed using a particle dynamics method. The vibration pattern of chosen particles on the surface was studied and its relation to the geometry of the fixed base region was investigated. The simulation results show systematic changes in signal form when processed with a similar HVSR method as a response to the shape of the fixed base.

Keywords: passive seismic, HVSR, particle dynamics, numerical modelling, LAMMPS

INTRODUCTION

The Earth's surface continuously experiences a background vibration, even in the absence of seismic activity. This phenomenon, known as ambient seismic noise (or microtremor), is generated by the dynamic interaction between the atmosphere, hydrosphere, and anthropogenic activities. The frequency spectrum of this vibration contains crucial information about the shallow subsurface structure [1]. A conventional method to process the ambient noise signal is the Horizontal to Vertical Spectral Ratio (HVSR) technique, popularized by Nakamura (1989) [2]. The technique calculates the spectral ratio of horizontal to vertical ground motion at a measurement point without the need for an active seismic source [3]. The method has been proven effective for estimating sediment thickness through site resonance frequencies and the inversion of the shear velocity (Vs30) [4].

In recent years, advancements in seismic ambient noise methods have further expanded the understanding of wavefield characteristics through passive seismic interferometry, enabling improved imaging of subsurface structures without active sources [5, 6]. Furthermore, the diurnal and anthropogenic influence on ambient noise frequency bands have been better characterized, enhancing the interpretation of HVSR data in urban and complex geological settings [7].

However, the interpretation of HVSR presents challenges due to its complexity. Spectral variations, such as sharp peaks or multi-modal behavior at adjacent locations, can indicate the influence of unobserved subsurface factors [1]. The work of Shahjouei & Pezeshk [8] and studies by Pischiutta [9] have demonstrated that basement geometry, sediment heterogeneity, and particle size distribution can significantly alter the spectral response. This uncertainty limits the accuracy of subsurface inverse modeling, particularly in areas with complex geological structures [10]. Recent studies by Pan & Ghofrani (2018) and D'Amico et al. (2020) further highlight the challenges of 2D/3D basin effects, showing that complex geometries can generate multiple resonance peaks that are difficult to interpret with conventional 1D models [11].

More recently, enhanced numerical simulations and urban ambient noise clustering approaches have been developed to better discriminate source mechanisms and analyze complex site amplification effects in heterogeneous environments [12]. These methods improve the resolution and interpretation of HVSR spectra, particularly in urbanized and basin settings.

To obtain more insight into the relationship between the spectral shape and the geometry of the base medium, an alternative modeling approach is needed that can capture the complex wave propagation and particle interactions in heterogeneous media more realistically than traditional continuum-based wave models. While wave propagation models are powerful, they often struggle to accurately represent the complex behavior of granular materials, such as non-linear effects and local interactions. Therefore, particle-based numerical simulations can be used. In this model, particles interact via a potential model that can be fitted to the physical characteristics of the modeled medium [1]. The vibration on the particles located at the surface will be influenced by the complex wave propagations inside the medium. By altering the

geometry of the bedrock in this particle-based framework, we can directly observe how a non-idealized, heterogeneous medium influences the HVSR spectral profile. The objective of this study is to find out the relation of the variation in bedrock geometry within a granular medium to the surface vibration through the HVSR spectral profile.

METHODS

This study was designed to understand how the geometry of the bedrock layer can influence vibration patterns at the surface. Through a series of controlled numerical simulations, this study evaluates the impact of variation in the bedrock contour on the dynamic response of the overlying material. Each step, from the model design to the analysis of the results, is systematically performed so that the influence of geometry can be directly observed and quantitatively compared against the characteristics of the resulting surface waves. This work was performed using the LAMMPS platform [13], a versatile molecular dynamics simulator widely adopted in materials and geosciences research for particle-based modeling at multiple scales, enabling detailed inter-particle interaction analysis [13, 14]. In this research, some bedrock shapes are simulated and the influence on the HVSR spectral pattern was observed. The data processing and visualization was performed using OVITO.

1. Numerical Model Design

1.1. General System Configuration

This study employs a two-dimensional (2D) granular system model composed of identical particles, interacting via the Lennard-Jones potential model. The system was configured within a simulation domain having periodic boundary conditions, which was applied in the horizontal direction. In that sense, the simulated bedrock structure is also periodic throughout the breadth of the simulation domain. The particles are initially placed in a close-packed hexagonal lattice configuration with uniform initial density. The reduced Lennard-Jonesian units were used, where distance is measured in standard reduced units based on Lennard-Jones potential parameters σ and ε, allowing for scalable and normalized simulation of particle interactions [13, 15]. This approach is widely adopted in molecular and granular dynamics simulations to capture fundamental particle behavior without explicit material specificity.

To address the relationship between the reduced Lennard-Jones (LJ) units used and real-world physical units, we note that these units are normalized based on the LJ potential parameters, namely σ (the zero-potential distance) and ϵ (the potential depth). This approach simplifies the calculations by allowing a focus on the general geometrical impact without being tied to specific material properties. While an explicit mapping to a specific geological medium is beyond the scope of this study, this methodology ensures our results can be qualitatively applied to different granular materials.

1.2. Variations in Geometry

To understand the influence of the bedrock surface shape, we chose three categories of geometric models. The first was a flat base model, which related to a flat bedrock geometry. In this case, variations were created by adjusting the bedrock's height, resulting in three different granular medium thicknesses—defined as the distance from the surface to the bedrock—of 9σ (for the lowest bedrock), 6σ, and 3σ (for the highest bedrock). The second category is a cone-shaped base model, representing a bedrock protrusion, which was simulated with three different cone base widths: 6σ, 11σ, and 15σ. The final category is a circular concave base model, which represents a basin-like depression, tested with three radii of curvature: 8σ, 14σ, and 20σ. A schematic representation of each model category is presented in FIGURE 1. The two last models represent the measure of roughness of the bedrock.

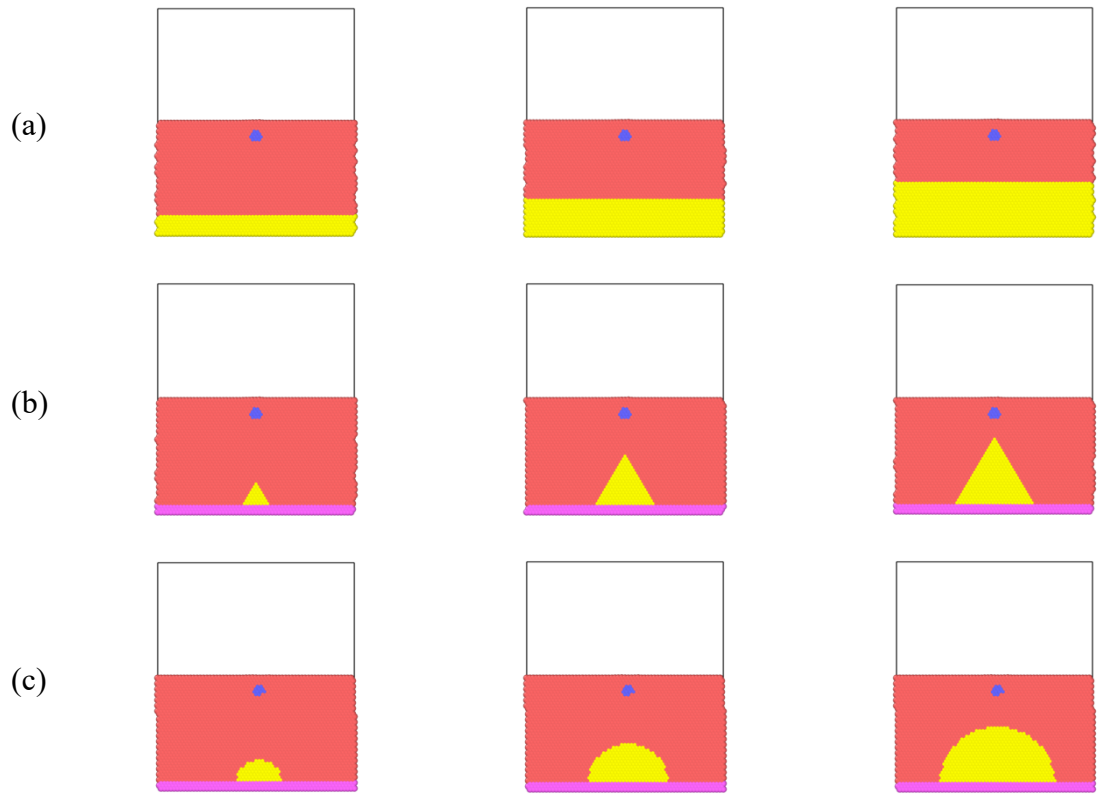

FIGURE 1. Schematic representation of the numerical models used in this study. (a) Flat base models with varying granular layer thicknesses of 3, 6, and 9 LJ units. (b) Cone-shaped base models with varying base radii of 5.6, 11.2, and 15.0 LJ units. (c) Concave base models with varying radii of curvature of 8, 14, and 20 LJ units. The blue dots represent the source of the disturbance.

2. Simulation Procedure with LAMMPS

Each model was constructed and executed using the Large-scale Atomic/Molecular Massively Parallel Simulator (LAMMPS), a software package specifically designed to efficiently perform large-scale particle-based simulations. LAMMPS enables high-performance complex numerical processing, making it ideally suited for this study to analyze the dynamic response of the various bedrock geometries [13].

2.1. Initialization and Equilibration

Once all particles are positioned, a constant vertical gravitational force is applied to the system. Subsequently, an equilibration phase is conducted to resolve any unrealistic particle overlaps. This step is critical to ensure that the system achieves a mechanically stable state before the main dynamic simulation is executed [16].

While it is ideal to run multiple simulations to ensure reproducibility, this study performed only a single simulation for each geometric scenario. Therefore, the presented results represent a single response from each model. This limitation means that the observed variations in the spectral response may be subject to random variability arising from the initial condition

2.2. Particle Simulation

Following the equilibration phase, the main simulation is performed. To mimic ambient vibrations, a select number of particles are assigned random initial velocities to act as noise source. The particles that were assigned as the noise source were given a specific temperature to ignite wave propagation inside the medium. Meanwhile, particles comprising the base layer and boundaries are held stationary by setting their net force to zero. The entire system is then evolved under the microcanonical (NVE) ensemble (constant number of particles, volume, and energy). Throughout the simulation, the position and velocity data for each particle are recorded at regular intervals for subsequent post-simulation analysis.

3. Physical Model and Parameters

3.1 Interparticle Interactions

The physical interaction between particles in this simulation is mathematically modeled using the Lennard-Jones (LJ) potential. This potential describes the attractive and repulsive forces that occur between two particles as a function of the distance between them. To enhance computational efficiency, a cut-off distance approach is used, where the interaction between particles is only taken into account if they are within a certain distance. The Lennard-Jones potential energy (U_{LJ}) as a function of the distance, r, between two particles is formulated as follows:

$$U_{LJ} = 4 \in \left[\left(\frac{\sigma}{r}\right)^{12} - \left(\frac{\sigma}{r}\right)^{6}\right].$$

FIGURE 2 schematically shows the potential energy curve for this model.

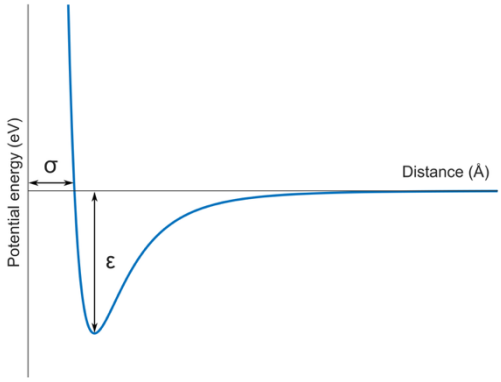

FIGURE 2. The Lennard-Jones (LJ) potential curve as a function of interparticle distance (r) [17].

As depicted by the Lennard-Jones potential graph, the curve clearly illustrates two types of interparticle interactions. At very short distances ($r < \sigma$), the potential energy rises sharply, resulting in a strong repulsive force. This force prevents particles from penetrating or overlapping one another. As the interparticle distance increases, the curve forms a potential well with a depth of $\in$, which represents an attractive force. This force maintains cohesion between particles within a certain range.

In the context of simulating dense granular materials, where particles are in contact or in very close proximity ($r \approx \sigma$), the most dominant interaction is the repulsive force. This steep repulsive force effectively serves as an approximation of the soft-sphere contact model [18]. To ensure the validity of the simulation results, all physical parameters in the interaction model—including $\in$ (potential depth), σ (zero-potential distance), and the cut-off distance—were kept identical for all models. This approach ensures that any observed differences in the wave response are attributable solely to the differences in the base geometry, and not to variations in material properties. The Lennard-Jones potential is widely accepted for modeling particle interactions in granular physics, capturing both adhesive and repulsive forces; its steep repulsive part effectively models contact forces in dense packings, while the potential well mimics cohesion effects [19].

3.2. Numerical Integration

The motion of particles in the system is governed by Newton's Second Law ($F = ma$), which states that a particle's acceleration is directly proportional to the net force acting upon it. Because this law is continuous in time, whereas computer simulations operate in discrete time steps (Δt), a numerical method is required to accurately integrate these equations of motion.

In this research, the Velocity-Verlet algorithm is used to perform the numerical integration. This algorithm was chosen for its high accuracy, good numerical stability, and its ability to conserve the system's energy over long-duration simulations [20]. This algorithm updates the position and velocity of each particle incrementally at each time step, Δt, through two main stages:

a. Position Update

The new particle position at time $t+\Delta t$ is calculated using the current position, velocity, and acceleration:

$$r(t+\Delta t) = r(t) + v(t)\Delta t + \frac{1}{2}a(t)\Delta t^2.$$

b. Velocity Update

After the position has been updated, the total force and the new acceleration, $a(t+\Delta t)$, are calculated. The particle's velocity is then updated using the average of the old and new accelerations:

$$v(t+\Delta t) = v(t) + \frac{a(t)+a(t+\Delta t)}{2}\Delta t.$$

4. Data Analysis and Visualization

The analysis of the simulation results was conducted through two complementary approaches to obtain a comprehensive understanding. First, a qualitative, visualization-based analysis was used to observe the physical behavior of the waves. Second, a quantitative analysis using the HVSR spectrum was applied to objectively measure the surface response.

4.1. Visualization and Qualitative Analysis with OVITO

To understand how waves propagate and interact with the various base geometries, the simulation output data were visualized using the Open Visualization Tool (OVITO) [21]. This process involved loading the data from LAMMPS, coloring the particles based on their velocity magnitude to highlight the wavefronts, and generating animations. Through this visual approach, complex phenomena such as wave reflection, diffraction, and focusing caused by the base topography could be directly observed. These observations served as an initial validation of the quantitative results, while also providing important physical context for the interpretation of the wave response. OVITO is widely used for scientific visualization and analysis of atomistic and particle simulation data, offering powerful real-time 3D rendering, pipeline-based data processing, and scripting capabilities that enhance understanding of complex simulation phenomena [21].

4.2. Quantitative Analysis with the HVSR Spectrum

The quantitative analysis in this study was performed by calculating the spectral ratio between the horizontal and vertical components of particle motion, known as the Horizontal to Vertical Spectral Ratio (HVSR) [2]. For this purpose, a custom script was developed in the Python environment with the aid of scientific libraries such as NumPy and SciPy. This approach allowed for efficient and flexible data processing, while also ensuring accuracy in the calculation of the resulting spectra and ratio.

a. Extraction and Preparation of Time Series Data

The first step in the HVSR analysis involves extracting particle motion data from the uppermost layer of the system, which represents the surface and acts as the primary wave receiver. This includes motion in the horizontal (x) and vertical (y) directions, along with timestep information from the simulation. The data is then reorganized chronologically to ensure continuity and accuracy in the time series, which is essential for the spectral transformation and HVSR calculation that follow.

b. Signal Processing: Windowing and Fourier Transform

To mitigate the effects of spectral leakage, a common artifact in the Fourier analysis of finite-duration signals, a Hamming window function was applied to both the horizontal and vertical component time series data. This function works by tapering the signal at its beginning and end, which results in a more accurate frequency spectrum representation. The Hamming window function, $w(n)$, for a signal of length N samples is defined as:

$$w(n) = 0.54 - 0.46\cos\left(\frac{2\pi n}{N-1}\right), \qquad 0 \le n \le N-1.$$

The original signal, $x(n)$, is multiplied by this function to produce the windowed signal, $x_{win}(n) = x(n) \cdot w(n)$. After windowing, the signal is transformed from the time domain to the frequency domain using the Fast Fourier Transform (FFT) algorithm, an efficient computational method for calculating the Discrete Fourier Transform (DFT). This transformation yields the complex spectrum, $X(k)$, which is subsequently converted into the amplitude spectrum, $S(f_k)$, by taking its absolute value:

$$X(k) = \sum_{n=0}^{N-1} x_{win}(n) e^{-i\frac{2\pi kn}{N}}, \qquad S(f_k) = |X(k)|.$$

This process is performed separately for the horizontal and vertical components, yielding the spectra $S_H(f)$ and $S_V(f)$, respectively. The zero-frequency component (DC offset) is removed, as it has no relevance in the context of dynamic vibrations.

c. HVSR Ratio Calculation and Spectral Smoothing

The HVSR ratio is obtained by dividing the horizontal amplitude spectrum, $S_H(f)$, by the vertical spectrum, $S_V(f)$. However, as both spectra often exhibit high fluctuations, the direct ratio calculation tends to be unstable. Therefore, a smoothing operation is first performed on each spectrum to emphasize the dominant patterns, particularly the fundamental frequency peak. The smoothing is performed using a one-dimensional Gaussian filter, which is mathematically equivalent to convolving the spectrum with a Gaussian function:

$$G(f) = \frac{1}{\sigma\sqrt{2\pi}} e^{-\frac{f^2}{2\sigma^2}}.$$

The parameter σ (the standard deviation) controls the degree of smoothing—a larger σ value results in a smoother spectral curve. This process effectively replaces each point in the spectrum with a weighted average of its neighboring points, with the weights determined by

the Gaussian function. After this process, the smoothed spectra, $S_{H,smooth}(f)$ and $S_{V,smooth}(f)$, are obtained. These are then used to calculate the final HVSR ratio via:

$$HVSR(f) = \frac{S_{H,smooth}(f)}{S_{V,smooth}(f)}.$$

This approach yields an HVSR curve that is more numerically stable and more accurately reflects the system's frequency response characteristics.

d. Comparative Analysis

The HVSR curves resulting from each geometric model were comparatively analyzed to evaluate the influence of the base topography on the vibrational response. The primary focus of this analysis was on two key spectral parameters: the fundamental peak frequency (f_0) and its corresponding peak amplitude (A_0). The fundamental peak frequency, f_0, is defined as the frequency at which the HVSR curve reaches its maximum value:

$$f_0 = \arg\max HVSR(f).$$

The peak amplitude, A_0, is the value of the HVSR at that frequency:

$$A_0 = HVSR(f_0) = \max\big(HVSR(f)\big).$$

According to site effects theory, f_0 reflects the natural resonant frequency of the sediment layer, while A_0 indicates the amount of ground motion amplification occurring at that frequency [22]. For an ideal case, such as a single, uniform layer of thickness H overlying a rigid bedrock, the theoretical value of f_0 can be estimated using the quarter-wavelength law:

$$f_0 = \frac{V_s}{4H},$$

where V_s is the average shear-wave velocity within the layer. This equation serves as a reference to validate the simulation results, especially for the flat base model. Meanwhile, any shifts in f_0 values and changes in A_0 that emerge in models with non-flat topography are analyzed as direct effects of the two-dimensional geometric variations.

RESULTS AND DISCUSSION

The results from the entire simulation suite are presented comparatively. FIGURE 3 displays the HVSR spectrum generated for each geometric model variation. Subsequently, the quantitative analysis via non-linear curve fitting is visualized in FIGURE 4.

Referring to FIGURE 3, unique spectral characteristics can be observed for each model category. For the flat base model (FIGURE 3a), the HVSR spectrum shows a clear and well-defined single peak, whose position shifts to lower frequencies as the layer thickness increases. The spectral characteristics change dramatically in the concave base model (FIGURE 3b), which produces a single, very sharp frequency peak with a much higher amplitude. In contrast, the cone-shaped base model (FIGURE 3c) displays the most complex frequency response, characterized by the appearance of multiple peaks (a multi-peak pattern).

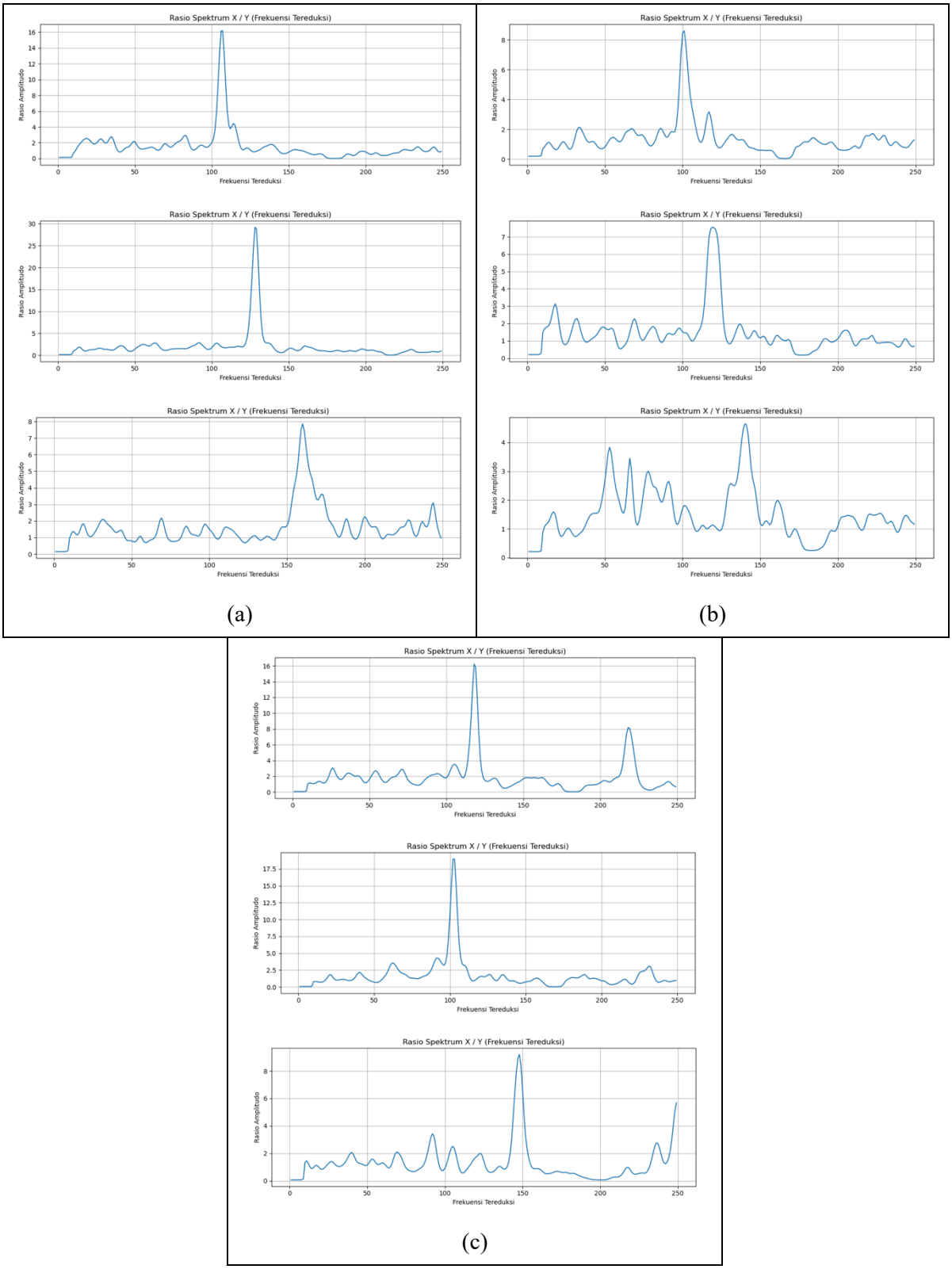

FIGURE 3. HVSR spectra for all simulated geometric models (a) Flat Base models with layer thicknesses of 3, 6, and 9 LJ units (from right to left). (b) Triangular Shaped Base models with base radii of 5.6, 11.2, and 15.0 LJ units (from right to left). (c) Concave Base models with radii of curvature of 8, 14, and 20 LJ units (from right to left).

The distinct spectral responses between the concave and cone-shaped models show the complexity of HVSR interpretation in the field. The concave model, which represents a sedimentary basin, shows a sharp and dominant resonance peak. This very sharp peak indicates a strong, focused resonance, where wave energy is trapped within the basin, a phenomenon known as the basin effect. This is consistent with the theory that geological basins can greatly amplify ground motion. The increase in amplitude at a single frequency can cause significant damage to structures built on top if their vibration frequency matches the natural frequency of the building [23].

The multi-peak response of the cone-shaped model is more complex to interpret. The appearance of several minor peaks is often ignored or considered noise. However, these simulation results show that these secondary peaks can be a natural response of irregular bedrock geometry, such as a bedrock hill or a thrust fault. Ignoring these peaks can lead to errors in determining the site resonance frequency f_0 and estimating sediment thickness [24]. For example, field surveys that show irregular HVSR peaks, such as in mountainous areas or with hard rock intrusions, are often a reflection of the subsurface geological complexity, not just a simple variation in sediment layer thickness [25].

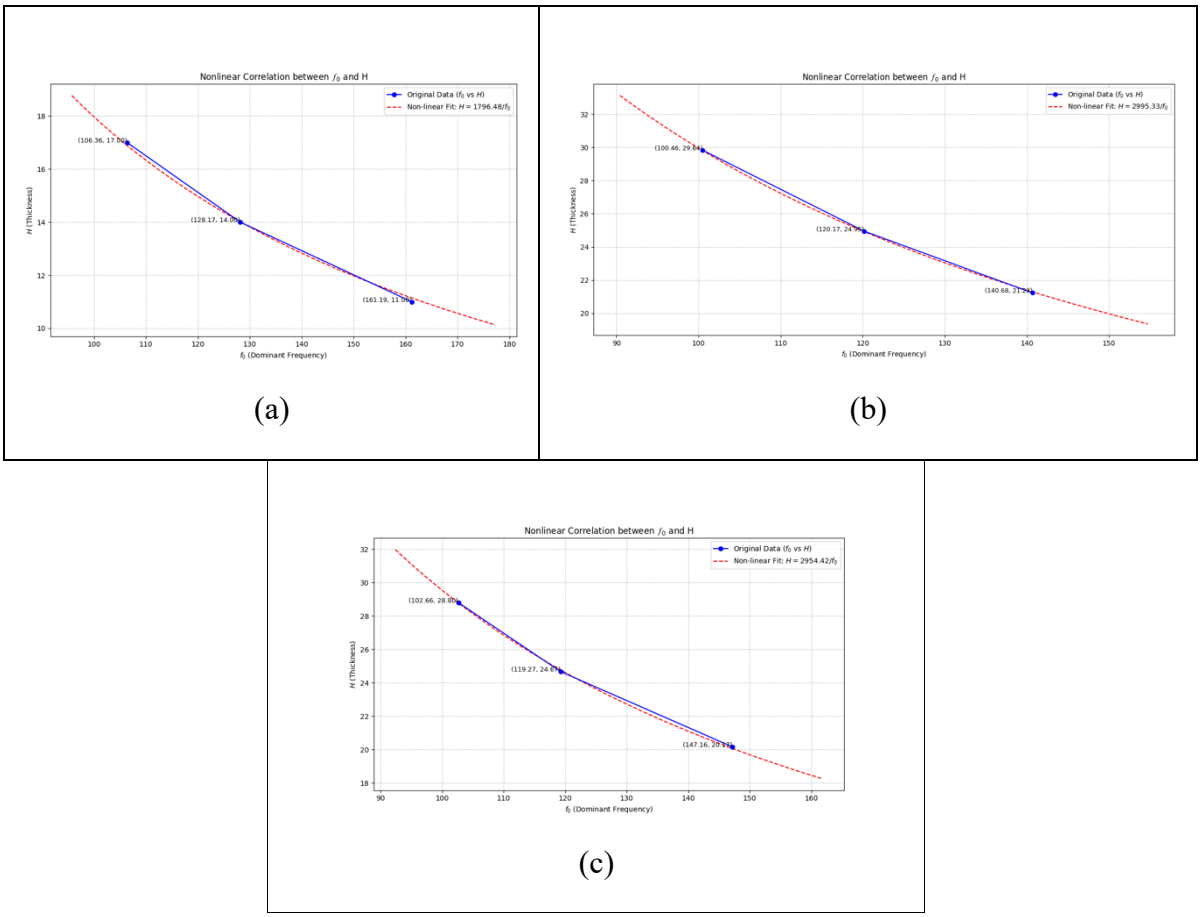

FIGURE 4. Non-linear curve fitting of the relationship between fundamental frequency and layer thickness for each model category: (a) Flat Base model, (b) Triangular Base model, and (c) Concave Base model.

The quantitative analysis, visualized in Figure 4, was performed to validate these trends. The theoretical basis used is the one-dimensional (1D) resonance equation, which states that the fundamental frequency (f_0) is related to the layer thickness (H) and the shear wave velocity (V_s) by the formula $f_0 = \frac{V_s}{4H}$. By rearranging this equation for the purpose of curve fitting, the model $H = \frac{V_s/4}{f_0}$ is obtained. In this form, the proportionality constant C is theoretically equivalent to the physical parameter $V_s/4$. The fitting of the simulation data yields three different values for the constant C for each geometric category. Using the relationship $V_s = 4 \times C$, three shear wave velocity values were obtained: 7185.92 for the flat base, 11981.32 for the cone base, and 11817.68 for the concave base (all in reduced LJ units).

CONCLUSION

This research concludes that the particle dynamics simulation results consistently demonstrate that the bedrock layer contour is a significant controlling factor of the vibrational response at the surface. This study identifies a strong correlation between the characteristics of the HVSR spectrum and two primary subsurface factors. First, an inverse relationship exists between the fundamental peak frequency (f_0) and the thickness of the sediment layer. Second, irregular bedrock geometry significantly modulates the response, leading to complex changes in both amplitude and dominant frequency. These findings underscore that the multiple spectral peaks often overlooked in the field can be direct indicators of complex bedrock topography. Therefore, disregarding these 2D/3D geometric effects can lead to inaccurate estimations of site resonance frequency (f_0) and shear wave velocity (Vs30), which has serious implications for seismic hazard assessment and geotechnical planning..

REFERENCES

[1] J. R. Peterson, "Observations and modeling of seismic background noise," US Geological Survey, 1993. doi: 10.3133/ofr93322.

[2] Nakamura, "A method for dynamic characteristics estimation of subsurface using microtremor on the ground surface," *Q. Rep. Rtri*, vol. 30, no. 1, pp. 25–33, Jan. 1989.

[3] SESAME, "Guidelines for the Implementation of the H/V Spectral Ratio Technique on Ambient Vibrations: Measurements, Processing and Interpretation." SESAME European Research Project WP12, 2004.

[4] M. W. Asten, A. Askan, E. E. Ekincioglu, F. N. Sisman, and B. Ugurhan, "Site characterisation in north-western Turkey based on SPAC and HVSR analysis of microtremor noise," *Explor. Geophys.*, vol. 45, no. 2, pp. 74–85, Jun. 2014, doi: 10.1071/EG12026.

[5] E. T. Y. Chang, Y. Gung, and Y. Chen, "Seismic Ambient Noise: Application to Taiwanese Data," in *Geophysical Monograph Series*, 1st ed., G. Bayrakci and F. Klingelhoefer, Eds., Wiley, 2024, pp. 17–29. doi: 10.1002/9781119750925.ch2.

[6] S. Molnar et al., "A review of the microtremor horizontal-to-vertical spectral ratio (MHVSR) method," *J. Seismol.*, vol. 26, no. 4, pp. 653–685, Aug. 2022, doi: 10.1007/s10950-021-10062-9.

[7] V. Shulakova, K. Tertyshnikov, R. Pevzner, Y. Kovalyshen, and B. Gurevich, "Ambient seismic noise in an urban environment: case study using downhole distributed acoustic sensors at the Curtin University campus in Perth, Western Australia," *Explor. Geophys.*, vol. 53, no. 6, pp. 620–633, Nov. 2022, doi: 10.1080/08123985.2021.2021802.

[8] A. Shahjouei and S. Pezeshk, "Alternative Hybrid Empirical Ground-Motion Model for Central and Eastern North America Using Hybrid Simulations and NGA-West2 Models," *Bull. Seismol. Soc. Am.*, vol. 106, no. 2, pp. 734–754, Apr. 2016, doi: 10.1785/0120140367.

[9] M. Pischiutta, M. Fondriest, M. Demurtas, F. Magnoni, G. Di Toro, and A. Rovelli, "Structural control on the directional amplification of seismic noise (Campo Imperatore, central Italy)," *Earth Planet. Sci. Lett.*, vol. 471, pp. 10–18, Aug. 2017, doi: 10.1016/j.epsl.2017.04.017.

[10] D. Fäh, F. Kind, and D. Giardini, "Inversion of local S-wave velocity structures from average H/V ratios, and their use for the estimation of site-effects," *J. Seismol.*, vol. 7, no. 4, pp. 449–467, Oct. 2003, doi: 10.1023/B:JOSE.0000005712.86058.42.

[11] S. Matsushima, T. Hirokawa, F. De Martin, H. Kawase, and F. J. Sanchez-Sesma, "The Effect of Lateral Heterogeneity on Horizontal-to-Vertical Spectral Ratio of Microtremors Inferred from Observation and Synthetics," *Bull. Seismol. Soc. Am.*, vol. 104, no. 1, pp. 381–393, Feb. 2014, doi: 10.1785/0120120321.

[12] K. Zhao, F. Cheng, J. Xia, J. Guan, and Z. Li, "Multistage deep clustering of urban ambient noise for seismic imaging—a case study for train-induced seismic noise," *Geophys. J. Int.*, vol. 242, no. 3, p. ggaf273, Jul. 2025, doi: 10.1093/gji/ggaf273.

[13] S. Plimpton, "Fast Parallel Algorithms for Short-Range Molecular Dynamics," *J. Comput. Phys.*, vol. 117, no. 1, pp. 1–19, Mar. 1995, doi: 10.1006/jcph.1995.1039.

[14] A. P. Thompson et al., "LAMMPS - a flexible simulation tool for particle-based materials modeling at the atomic, meso, and continuum scales," *Comput. Phys. Commun.*, vol. 271, p. 108171, Feb. 2022, doi: 10.1016/j.cpc.2021.108171.

[15] C. Y. Maghfiroh, A. Arkundato, Misto, and W. Maulina, "Parameters (σ, ε) of Lennard-Jones for Fe, Ni, Pb for Potential and Cr based on Melting Point Values Using the Molecular Dynamics Method of the Lammps Program," *J. Phys. Conf. Ser.*, vol. 1491, no. 1, p. 012022, Mar. 2020, doi: 10.1088/1742-6596/1491/1/012022.

[16] C. L. Brooks, "Computer simulation of liquids: By M. P. Allen (University of Bristol) and D. J. Tildesley (Southampton University). Clarendon Press, Oxford, UK; Oxford University Press, New York; 1987.xix+385 pp. ISBN 0470-20812-0," *J. Solut. Chem.*, vol. 18, no. 1, pp. 99–99, Jan. 1989, doi: 10.1007/BF00646086.

[17] B. Colas, "Structural Constraints on the Crystallisation of Amorphous Calcium Carbonate," 2017, doi: 10.13140/RG.2.2.20572.08327.

[18] P. A. Cundall and O. D. L. Strack, "A discrete numerical model for granular assemblies," *Géotechnique*, vol. 29, no. 1, pp. 47–65, Mar. 1979, doi: 10.1680/geot.1979.29.1.47.

[19] N. Bell, Y. Yu, and P. J. Mucha, "Particle-based simulation of granular materials," in *Proceedings of the 2005 ACM SIGGRAPH/Eurographics symposium on Computer animation*, Los Angeles California: ACM, Jul. 2005, pp. 77–86. doi: 10.1145/1073368.1073379.

[20] W. C. Swope, H. C. Andersen, P. H. Berens, and K. R. Wilson, "A computer simulation method for the calculation of equilibrium constants for the formation of physical clusters of molecules: Application to small water clusters," *J. Chem. Phys.*, vol. 76, no. 1, pp. 637–649, Jan. 1982, doi: 10.1063/1.442716.

[21] A. Stukowski, "Visualization and analysis of atomistic simulation data with OVITO–the Open Visualization Tool," *Model. Simul. Mater. Sci. Eng.*, vol. 18, no. 1, p. 015012, Jan. 2010, doi: 10.1088/0965-0393/18/1/015012.

[22] K. Konno and T. Ohmachi, "Ground-motion characteristics estimated from spectral ratio between horizontal and vertical components of microtremor," *Bull. Seismol. Soc. Am.*, vol. 88, no. 1, pp. 228–241, Feb. 1998, doi: 10.1785/BSSA0880010228.

[23] D. Badode, D. V. Varghese, A. Nikhade, and D. S. Shirkhedkar, "SITE SPECIFIC STUDY OF SEISMIC HAZARD ANALYSIS – CASE STUDY REVIEW," vol. 05, no. 05, 2021.

[24] S. Molnar et al., "A review of the microtremor horizontal-to-vertical spectral ratio (MHVSR) method," *J. Seismol.*, vol. 26, no. 4, pp. 653–685, Aug. 2022, doi: 10.1007/s10950-021-10062-9.

[25] J. L. De Guevara et al., “Ambient Noise H / V Spectral Ratio in Site Effect Estimation in La Mesa de Macaracas, Panama,” *Int. J. Geophys.*, vol. 2022, pp. 1–10, Mar. 2022, doi: 10.1155/2022/6171529.